EUROPEAN SOCIETY OF RADIOLOGY

European Radiology
EXPERIMENTAL

ORIGINAL ARTICLE

Open Access

7-T MRI-based surrogate for histopathology examination of liver fibrosis

Jérémy Dana[1,2,3,4], Antonin Fattori[5], Chrystelle Po[6], Aurélie Beaufrère[7], Valérie Vilgrain[8], Valérie Paradis[7], Patrick Pessaux[1,9], Thomas F. Baumert[1,2,10], Benoît Gallix[3,11,12] and Aïna Venkatasamy[6,13,14]*

Abstract

Background To demonstrate that 7-T magnetic resonance imaging (MRI) provides a surrogate for histopathology of fresh *ex vivo* liver tissue, using the case study of liver fibrosis.

Methods We prospectively enrolled 20 patients undergoing surgical liver resection between November 2021 and April 2023. Each *ex vivo* fresh liver tissue specimen (~ 1 cm^3) was sectioned in half. The first half, stained using Masson's Trichrome and Perls, was assessed by three pathologists using the METAVIR score (reference standard). The second half was imaged with 7-T MRI using a cryoprobe (fat-suppressed T2-weighted turbo/fast spin-echo sequence, spatial resolution $75 \times 75 \times 200$ μm^3) and assessed by three radiologists and the same three pathologists, using a newly developed MRI-METAVIR score.

Results Five patients were excluded from the final analysis (one patient due to poor specimen quality, two due to surgery cancellation, and two previously published used for reader training). Of the remaining 15 patients, 10 (67%) presented with chronic liver diseases and 8/15 (53%) with advanced (F3 or F4) fibrosis. Radiologists achieved 88% sensitivity, 100% specificity, 93% accuracy (95% confidence interval 68–100%) and 0.94 Harrell's c-index (0.86–1.00). Pathologists achieved 88% sensitivity, 86% specificity, 87% accuracy (60–98%) and 0.87 Harrell's c-index (0.74–0.99). There were no statistically significant differences between MRI-based and pathologic reference standard stage ($p \geq 0.655$).

Conclusion With an in-plane spatial resolution of ~ 75×75 μm^2, MRI paralleled low-magnification histology, enabling the assessment of micro-architectural liver changes, and provided a surrogate for histopathology examination of fresh *ex vivo* liver tissue samples at a microscopic level.

Relevance statement 7-T MRI provides a surrogate for histopathology visualisation of fresh *ex vivo* liver tissue, opening new research perspectives for clinical high-field MRI of the liver.

Key Points

- Using the newly developed MRI-METAVIR score, 7-T MRI data strongly correlated with histopathology, achieving excellent agreement and accuracy.
- 7-T MRI accurately differentiated advanced from minimal liver fibrosis.
- 7-T MRI visualises liver micro-architecture, enabling pathology-like, noninvasive three-dimensional imaging.

Keywords Hepatitis, Histopathology, Liver diseases, Liver fibrosis, Magnetic resonance imaging

*Correspondence:
Aïna Venkatasamy
aina.vnkt@gmail.com
Full list of author information is available at the end of the article
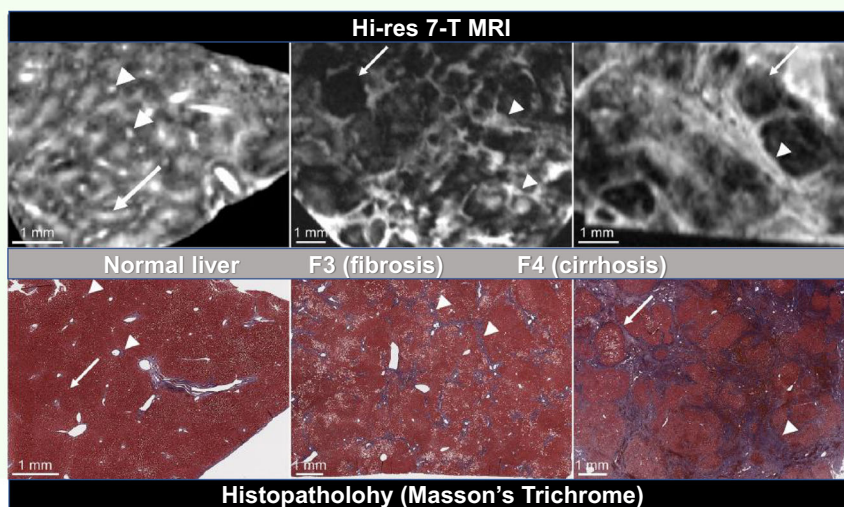
Springer Open

Graphical Abstract

7-T MRI-based surrogate for histopathology examination of liver fibrosis

ESR | EUROPEAN SOCIETY OF RADIOLOGY

High-resolution 7-T MRI:
- correlates strongly with histopathology, achieving excellent agreement and accuracy.
- distinguishes advanced fibrosis (F3-F4) from minimal fibrosis (F0-F1).
- visualises liver microarchitecture, enabling pathology-like, non-invasive 3D imaging.

7-T MRI achieves a histopathology-like visualisation of fresh *ex-vivo* liver tissue, comparable to low-magnification histology

Hi-res 7-T MRI

Normal liver | F3 (fibrosis) | F4 (cirrhosis)

Histopatholohy (Masson's Trichrome)

European Radiology EXPERIMENTAL

Eur Radiol Exp (2025) Dana J, Fattori A, Po C et al; DOI: 10.1186/s41747-025-00589-8

Background

Histopathological examination, the standard of care for tissue analysis, requires intricate technical processes for tissue preparation, which inevitably delay the availability of results by at least 12 h following tissue sampling, rendering it unsuitable for intraoperative decision-making [1]. Extemporaneous histopathological examination, which employs an alternative technical procedure, enables a reduction in turnaround time, yielding preliminary results in less than 30 min [2]. However, these alternative procedures involve a freezing step and are responsible for tissue alterations such as morphological artefacts and sample exhaustion. Additionally, histopathological examination of liver biopsies is also prone to sampling errors [3] and/or inter-reader variability [4]. Although rare, liver biopsies are invasive with risks of bleeding complications [5].

High-field magnetic resonance imaging (MRI), with recent improvements such as radiofrequency coils, sequence optimisation, and imaging postprocessing [6], is now able to reach a very high spatial resolution, approximating that of histology (*i.e.*, < 100 μm, compared to ~ 1 mm for clinical MRI) and appears as a promising tool to image fresh *ex vivo* tissues [7, 8]. Several studies reported the potential of high-field MRI for a pathology-like analysis of resected breast and lymphatic tissue on fresh *ex vivo* tissue samples [7, 9]. Similarly, the potential of this tool to provide pathology-like images was previously confirmed on two *ex vivo* liver samples [8]. Additionally, MRI is a noninvasive imaging modality, without the incompressible tissue processing time required for histology, with limited tissue preparation. High-field MRI appears as a promising "missing link" between conventional imaging and histology.

Liver fibrosis is characterised by the accumulation of extracellular matrix proteins caused by sustained liver insults. It is the inevitable consequence of all progressive chronic liver disease, ultimately leading to cirrhosis with complications such as hepatocellular carcinoma and portal hypertension. Liver fibrosis appears as an appropriate model for exploring high-resolution MRI because of the existence of widely validated histological classifications of liver fibrosis, with low subjectivity, such as the METAVIR system score used to classify the liver tissue on Masson's trichrome-stained sections into five levels, from F0 to F4 [10–15].

This study aims to demonstrate that high-field MRI provides an accurate surrogate for histopathology examination of fresh *ex vivo* tissue using the case study of liver fibrosis on surgical liver samples.

Dana *et al. European Radiology Experimental* (2025)9:54

Page 3 of 10

Methods

This prospective project was approved by the Research Ethics Board (Protocol RIPH2, LivMod N°IDRCB 2019-A00738-49 ClinicalTrial NCT04690972) and followed ethical principles of the Declaration of Helsinki. All patients provided written informed consent.

Study design

This prospective study enrolled twenty patients aged > 18 years, who underwent surgical liver resection between November 2021 and April 2023. The overall study workflow is presented in Fig. 1. We used *ex vivo* fresh liver tissue (~ 1 cm^3) from surgically resected livers. Each fragment was sectioned in half, and the sections were identified, so that the MRI acquisition plane was as close as possible to the histological one. We imaged the first half, placed in Fluorinert™ Electronic Liquid FC40 (Sigma-Aldrich, Overijse, Belgium), a nonconductive, thermally and chemically stable fluid without ^{1}H signal, using a 7-T MRI system with a cryoprobe (Bruker BioSpin, Rheinstetten, Germany). T2-weighted fat-suppressed turbo/fast spin-echo images were acquired with a rapid imaging with refocused echoes (RARE) sequence, whose parameters are summarised in Table 1. The cryoprobe technology employs cryogenically cooled radiofrequency coils and amplifiers cooled by a closed-cycle refrigeration system, allowing the reduction of electronic noise. The second half was fixed in formalin, embedded in paraffin, cut at a 4-μm thickness in the same plane as the MRI acquisition, and then stained using Masson's Trichrome and Perls. The minimum processing time for pathology samples was around 48 h. All histology slides were digitally scanned using the Ventana DP 200 slide scanner (Roche, Basel, Switzerland). The low magnification used ranged between 1× and 2×, depending on the sample, and the scale bar was indicated for each microphotograph.

### Assessment of MRI and pathology images

Three subspecialty-trained abdominal radiologists (B.G., V.V., and A.V., with 27, 35, and 7 years of experience, respectively) and three subspecialty-trained abdominal pathologists (A.F., V.P., and A.B. with 5, 30, and 10 years of experience) assessed both MRI and pathology images, independently and blinded to medical records. The readings of MRI and pathology images were conducted in two separate sessions, over a month apart.

Pathology images

In the first session, the three pathologists independently staged fibrosis on digital histological slides according to the METAVIR score using the software QuPath® [16]. The consensus fibrosis stage for pathology was based on the agreement of at least two of the three pathologists.

MRI

The second session consisted of the reading of MRI images using 3D Slicer [17], the cases being presented in a different random order, by all three radiologists and three pathologists, given that this new field of application is halfway between the two specialities. First, all readers (radiologists and pathologists) received training on the METAVIR classification of fibrosis and the semiology of the fibrosis on high-field MRI (MRI-METAVIR score as described below), using two previously published cases [8]
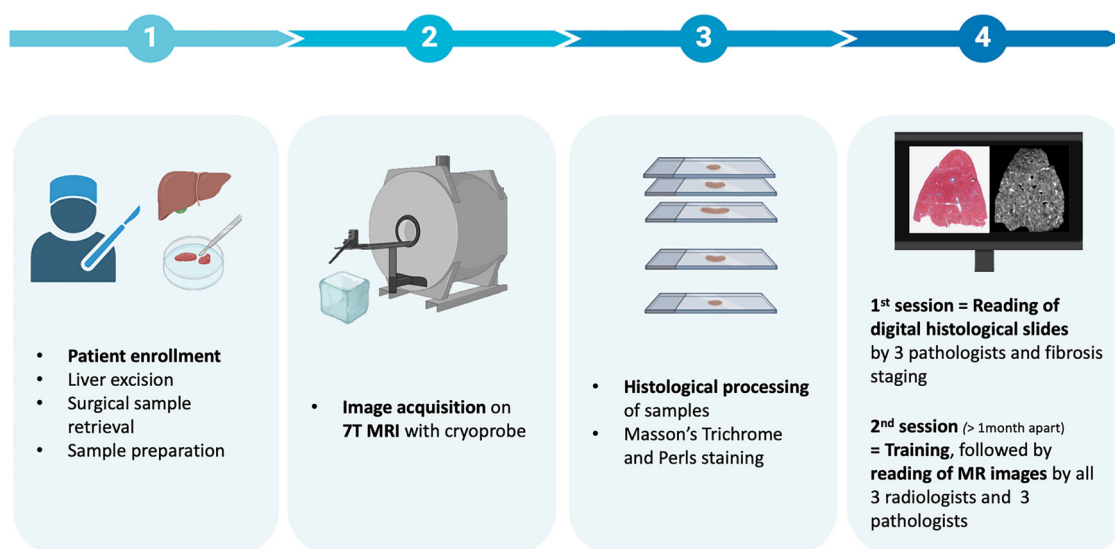
Fig. 1 Schematic diagram of the overall workflow of the study

Dana *et al. European Radiology Experimental* (2025)9:54

Page 4 of 10

Table 1 Sequence parameters for the rapid imaging with refocused echoes (RARE) T2-weighted sequence

Repetition time (ms)	Echo time (ms)	Number of excitations	RARE factor	Matrix	Slice thickness (µm)	Field-of-view (mm)	Spatial resolution (µm)	Acquisition time (min)
3,000	30	25	2	266 × 200 × 42	200	20 × 15 × 6	75 × 75 × 200	240

and schematic illustrations of high-field MRI for each stage (F0 to F4, Fig. 2). Then, all reviewers were asked to review the MRI images (6 images per patient) and stage fibrosis, according to the MRI-METAVIR score. The consensus fibrosis stage for MRI was based distinctively on the agreement of at least 2 two of the three radiologists and on the agreement of at least two of the three radiologists. To create the MRI-METAVIR score, one subspecialty-trained abdominal radiologist who did not participate in the reading (J.D., with 3 years of experience) reviewed all MRI images and analysed the MRI features of fibrosis in correlation with their corresponding histological section. The MRI-METAVIR score has been developed in analogy with the histological staging criteria, based on the presence and distribution of fibrosis [8].

Reference standard
The reference standard was the consensus fibrosis METAVIR stage based on the agreement of at least two of the three pathologists using the pathology images only.

Endpoint
The endpoint of the study was the performance of 7-T MRI to diagnose advanced fibrosis (stage F3 or F4) in fresh *ex vivo* liver tissue using the newly developed MRI-METAVIR score.

Statistical analysis
Performance metrics of MRI were computed for sensitivity, specificity, accuracy, positive and negative predictive values, area under the receiver operating characteristic curve, and c-index. Paired ordinal non-normally distributed data were compared with the Wilcoxon signed-rank test. The concordance between the pathologic gold standard and the MRI consensus was calculated using weighted κ (linear weights). The inter-reader agreement was calculated using Fleiss κ [18]. The agreement was interpreted according to κ values as follows: < 0.00 (poor); 0.00–0.20 (slight); 0.21–0.40 (fair); 0.41–0.60 (moderate); 0.61–0.80 (substantial); 0.81–1.00 (almost perfect) [19]. All statistical analysis was performed using MedCalc Statistical Software version 23.0.5 (MedCalc Software bv, Ostend, Belgium; https://www.medcalc.org) and SPSS Statistics version 29 (IBM, IBM Corporation, New York, USA).
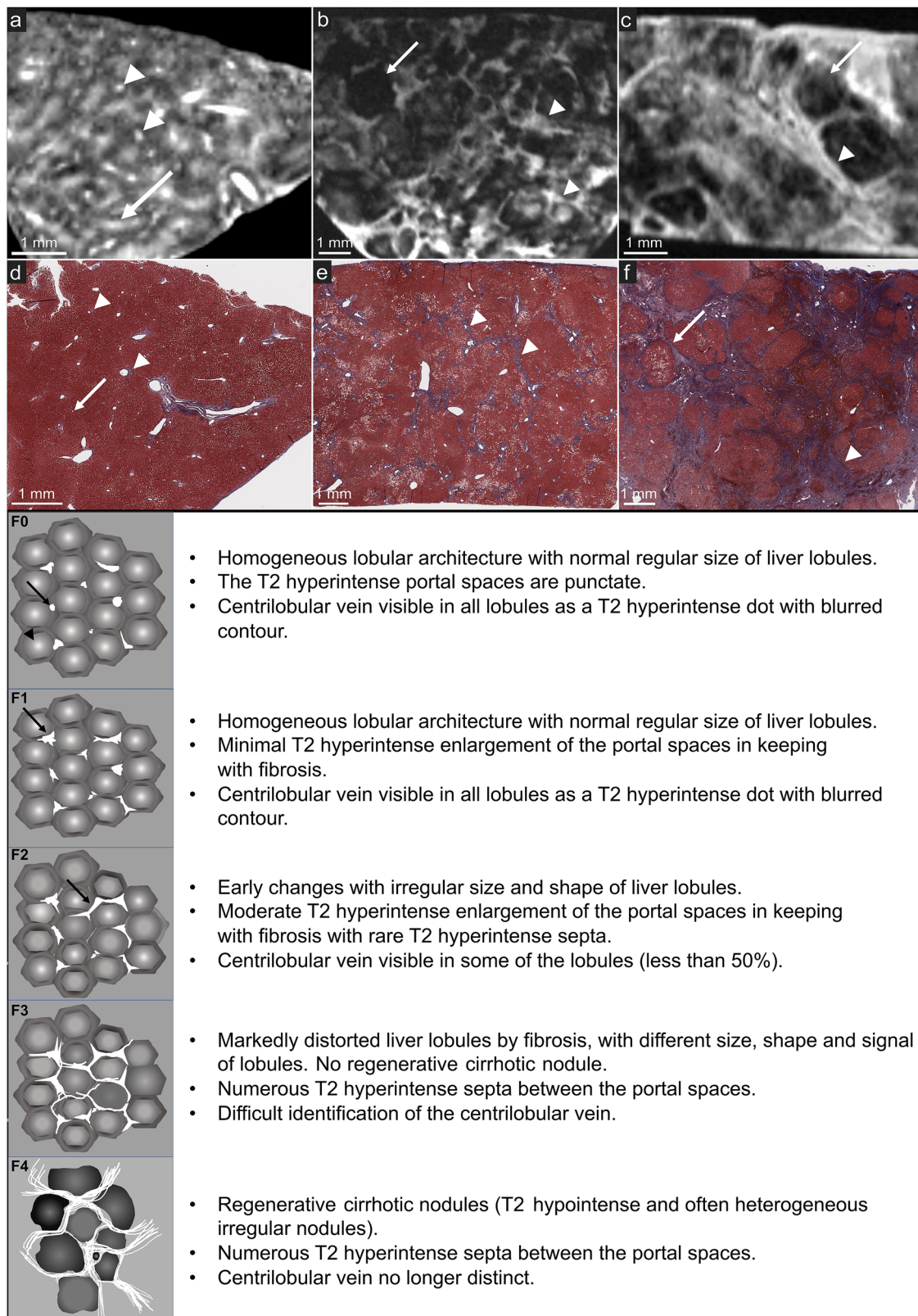
Results

Population
A total of 20 consecutive patients scheduled for liver surgery were included in the study. There was no adverse event or complication during the specimen collection or MRI procedure. Three patients were excluded due to poor specimen quality, not allowing MRI or pathology examination ($n = 1$) and cancellation of the surgery ($n = 2$). In addition, two of the 20 included patients, previously published [2], were used for reader training and not included in the final dataset. The final dataset consisted of 15 patients, 12 men and 3 women, with a median age of 68 years, interquartile range 60–73, who underwent liver surgery for primary liver lesions ($n = 10$) or colorectal cancer liver metastases ($n = 5$). Chronic liver disease of several aetiologies was present in 10 of 15 patients (67%) (Table 2).

The pathologists' consensus results for fibrosis staging on Masson's Trichrome-stained slides, which served as a reference standard, were as follows: 2 of 15 patients (13%) had a METAVIR stage of F0, 5 (33%) of F1, 5/15 (33%) of F3, and 3/15 (20%) of F4 (Table 1). In all cases, no consensus review was necessary, and the agreement between the pathologists regarding the review of histopathology images was very good (κ = 0.77, 95% confidence interval (CI) 0.61–0.93).

Accuracy of MRI
The diagnostic performances of MRI for a histopathology-like diagnosis of the absence (F0) or very early (F1) fibrosis, and the presence of advanced fibrosis (F3 or F4), were excellent for both radiologists and pathologists (Table 3, Fig. 2). Radiologists achieved an 88% sensitivity (95% CI 47–100%), 100% specificity (59–100%), 100% positive predictive value (59–100%), 88% negative predictive value (95% CI 53–98%), 93% accuracy (95% CI 68–100%), 0.94 AUC (95% CI 0.69–1.0) and 0.94 Harrell's c-index (95% CI 0.86–1.0). Pathologists achieved 88% sensitivity (95% CI 47–100%), 86% specificity (95% CI 42–100%), 88% positive predictive value (95% CI 53–98%), 86% negative predictive value (95% CI 48–98%), 87% accuracy (95% CI 60–98%), 0.87 AUC (95% CI 0.60–0.98%), and 0.87 Harrell's c-index (95% CI 0.74–0.99). There were no statistically significant differences between MRI stages and pathologic gold standard

F0
- Homogeneous lobular architecture with normal regular size of liver lobules.
- The T2 hyperintense portal spaces are punctate.
- Centrilobular vein visible in all lobules as a T2 hyperintense dot with blurred contour.

F1
- Homogeneous lobular architecture with normal regular size of liver lobules.
- Minimal T2 hyperintense enlargement of the portal spaces in keeping with fibrosis.
- Centrilobular vein visible in all lobules as a T2 hyperintense dot with blurred contour.

F2
- Early changes with irregular size and shape of liver lobules.
- Moderate T2 hyperintense enlargement of the portal spaces in keeping with fibrosis with rare T2 hyperintense septa.
- Centrilobular vein visible in some of the lobules (less than 50%).

F3
- Markedly distorted liver lobules by fibrosis, with different size, shape and signal of lobules. No regenerative cirrhotic nodule.
- Numerous T2 hyperintense septa between the portal spaces.
- Difficult identification of the centrilobular vein.

F4
- Regenerative cirrhotic nodules (T2 hypointense and often heterogeneous irregular nodules).
- Numerous T2 hyperintense septa between the portal spaces.
- Centrilobular vein no longer distinct.

Fig. 2 (See legend on next page)

(see figure on previous page)

Fig. 2 Schematic illustrations of the MRI-METAVIR score with high-resolution liver magnetic resonance imaging and histopathology correlation (Masson's Trichrome) in a normal liver (**a**, **d**), F3 liver T2 (**b**, **e**), and F4 (cirrhosis) liver (**c**, **f**). On **a** and **d**, the liver architecture is homogeneous with hyperintense punctate portal spaces (arrow) and centrilobular veins (arrowhead). On **b** and **e**, the liver architecture is distorted by numerous T2 hyperintense fibrotic septa (arrowhead) with lobules of different size, shape, and signal (arrow). On **c** and **f**, there are regenerative cirrhotic nodules (arrow) separated by fibrotic septa (arrowhead)

Table 2 Demographics, clinical characteristics, surgical indications, and results of consensus review of pathology slides and 7-T magnetic resonance imaging fibrosis staging

Age (years)	Sex	Chronic liver disease	Surgical indication	Pathological fibrosis stage	MRI fibrosis stage
59	M	Hepatitis B and C viruses	Hepatocellular carcinoma	F2	Training
49	F	None	Metastases	F0	Training
73	M	MASLD	Hepatocellular carcinoma	F1	F0
57	M	Indeterminate aetiology	Metastases	F3	F2
73	M	None	Metastases	F0	F0
64	M	MetALD (MASLD and increased alcohol intake)	Hepatocellular carcinoma	F3	F3
58	M	None	Biliary cystadenoma	F1	F1
65	M	Alcohol associated liver disease	Hepatocellular carcinoma	F4	F4
73	M	MetALD (MASLD and increased alcohol intake)	Hepatocellular carcinoma	F1	F1
72	F	Alcohol associated liver disease	Hepatocellular carcinoma	F3	F4
71	M	None	Metastases	F1	F0
62	M	Alcohol associated liver disease	Hepatocellular carcinoma	F4	F4
56	F	None	Metastases	F0	F0
68	M	Indeterminate aetiology	Hepatocellular carcinoma	F3	F3
60	F	None	Metastases	F1	F1
68	M	Alcohol associated liver disease	Hepatocellular carcinoma	F3	F4
80	M	MASLD	Hepatocellular carcinoma	F4	F4

F Female, *M* Male, *MASLD* Metabolic dysfunction-associated steatotic liver disease

stages ($p = 0.655$ for radiologists and $p = 1.000$ for pathologists). MRI correctly classified 7 of 8 patients with advanced fibrosis on pathology (1 patient was staged F2 on MRI but was F3 on histopathology). Conversely, MRI correctly excluded fibrosis (*i.e.*, F0 or F1 stages) in 7 of 7 compared to histopathology. The concordance of MRI analysis with histopathology was excellent for radiologists ($\kappa = 0.81$; 95% CI 0.67–0.95) and moderate for pathologists ($\kappa = 0.50$; 95% CI 0.26–0.73) for all fibrosis stages. Figure 3 shows a discordant case between MRI assessment and histopathologic gold standard.

The inter-reader agreement between the six readers was moderate ($\kappa = 0.42$; 95% CI 0.29–0.55), fair between the three radiologists ($\kappa = 0.32$; 95% CI 0.29–0.61) but almost perfect between the three pathologists ($\kappa = 0.82$; 95% CI 0.53–1.00).

Discussion

High-field 7-T MRI demonstrated excellent performance in accurately staging liver fibrosis compared to histopathology, highlighting its potential as an innovative surrogate or complementary tool for low-magnification histology. Indeed, this study showed that the 7-T MRI can provide sufficient contrast between tissues to enable histopathology-like examination without the need for staining [7, 8]. In addition, MRI has the undeniable advantage over histology of being able to acquire images in a relatively short time with immediate image interpretation, as with any routine MRI. The specimen, which remains intact, can still be processed for pathologic examination afterward [7, 8].

Reaching very high in-plane spatial resolution ($\sim 75 \times 75\ \mu m^2$), close to that of low-magnification histology [20], MRI provided a completely new insight into the imaging of the liver architecture, which would not have been visible with the in-plane spatial resolution of a clinical standard MRI ($\sim 1\ mm^2$) [21, 22]. Fibrotic changes to the liver parenchyma observed on Masson's trichrome-stained histology slides were readily depictable on high-field MRI, appearing as T2-weighted hyperintense septa [8, 21, 22] together with fibrosis-related micro-architectural distortions at early stages [23]. While MRI has indeed a lower spatial resolution compared to histology, it provides a comprehensive assessment of liver

Table 3 Diagnostic performances and concordance (weighted κ) of MRI with pathologic reference standard to identify and stage hepatic fibrosis and inter-reader agreement

	Inter-reader agreement	Agreement with pathologic reference standard			
		Ratio	Accuracy	Harrell's c-index	Weighted κ
Radiologists					
No or very early fibrosis (F0-F1)	κ = 0.32 [0.29–0.61]	7/7	93% [68–100%]	0.94 [0.86–1.00]	κ = 0.87 [0.62–1.0]
Advanced fibrosis (F3-F4)		7/8			
Pathologists					
No or very early fibrosis (F0-F1)	κ = 0.82 [0.53–1.00]	6/7	87% [60–98%]	0.87 [0.74–0.99]	κ = 0.73 [0.39–1.0]
Advanced fibrosis (F3-F4)		7/8			

Inter-reader agreement was calculated using Fleiss κ. 95% confidence intervals in squared brackets

micro-architecture, enabling the evaluation of fibrosis-related structural changes, beyond the limitations of two-dimensional histological slices. Unlike histology, which relies on two-dimensional sectioning, MRI allows for the evaluation of larger and intact tissue volumes, minimising sampling bias and preserving the native tissue structure, without the need for fixation or staining [7, 8]. Although histology remains the standard of care, it is subject to tissue-processing artifacts and sampling bias, whereas MRI provides a more comprehensive imaging.

Regarding the choice of MRI sequence, T2-weighted RARE provided an optimal balance between high in-plane spatial resolution ($75 \times 75\ \mu m^2$) and contrast resolution, allowing detailed visualisation of liver micro-architecture and fibrotic tracts. Thus, the spatial resolution was optimised by adjusting acquisition parameters to maximise signal-to-noise ratio while maintaining a reasonable scanning time to prevent sample degradation.

While consensus MRI results were excellent, the inter-reader agreement between radiologists was poorer than that of pathologists. This was expected as the three radiologists had no experience with these images prior to this reading. Their only training consisted of a session based on two previously published pathological images and schematic representations, which were not representative of all stages of fibrosis. This was done to keep as many cases as possible in the final reading set. Of note, when the METAVIR score was first used by pathologists, its interobserver reproducibility was also poor [24].

The main limitation of this proof-of-concept study is the limited number of patients without any patients with F2 stage fibrosis. However, Dana et al [8] reported a case of F0 *versus* F2 accurate staging on high-field MRI, which also highlights the promising potential of the MRI-METAVIR score. Although these findings should be confirmed in a more extensive cohort, the number of expert reviewers for MRI and histology images strengthens the validity of the MRI-METAVIR score. On the other hand, the limited number of patients did not represent the full spectrum of liver conditions. Also, in case of iron overload in the liver, there is shortening of T2/T2* relaxation times, which is even worsened at 7 T, which can result in decreased signal-to-noise ratio [25]. Similarly, a fixed echo time could also influence contrast in cases of hepatic steatosis, and future studies are required to address this more specifically. In addition, although the samples were placed in Fluorinert™ Electronic Liquid FC40, a nonconductive, thermally and chemically stable fluid without ^{1}H signal, the limited number of patients did not allow us to investigate the impact of the specific absorption rates and excessive heat on the samples. Another limitation is the very low number of cases ($n = 2$) in the training set, related to sample availability. Despite this limitation, the diagnostic performance of radiologists to accurately stage fibrosis did not appear to have been significantly impacted (sensitivity 88%, specificity 100%).

This study paves the way for further applications of this technique to organs other than the liver. By offering direct, pathology-like access to the micro-architecture of *ex vivo* tissue samples, high-field MRI opens up a range of new applications. This noninvasive technique broadens the scope of tissue imaging possibilities of liver, brain, brainstem, lymph nodes, or atherosclerotic plaque [7, 9, 26–28]. In surgical oncology, this technique would be particularly useful for a simplified, noninvasive, real-time analysis of surgical specimens. For instance, several attempts to assess the *ex vivo* lymph node metastatic status in breast cancer yielded promising results despite long acquisition time [7, 9]. Similarly, oncological surgeries requiring extemporaneous analysis of tissues could also benefit from this nondestructive analysis to assess tumour margins (*e.g.*, partial nephrectomy, bronchial resection margins in lung cancer surgery) where the margins of a tumour could be rapidly assessed in their entirety as a three-dimensional volume without specific preparation (*i.e.*, including cutting) the specimen.

Dana *et al. European Radiology Experimental* (2025)9:54

Page 8 of 10
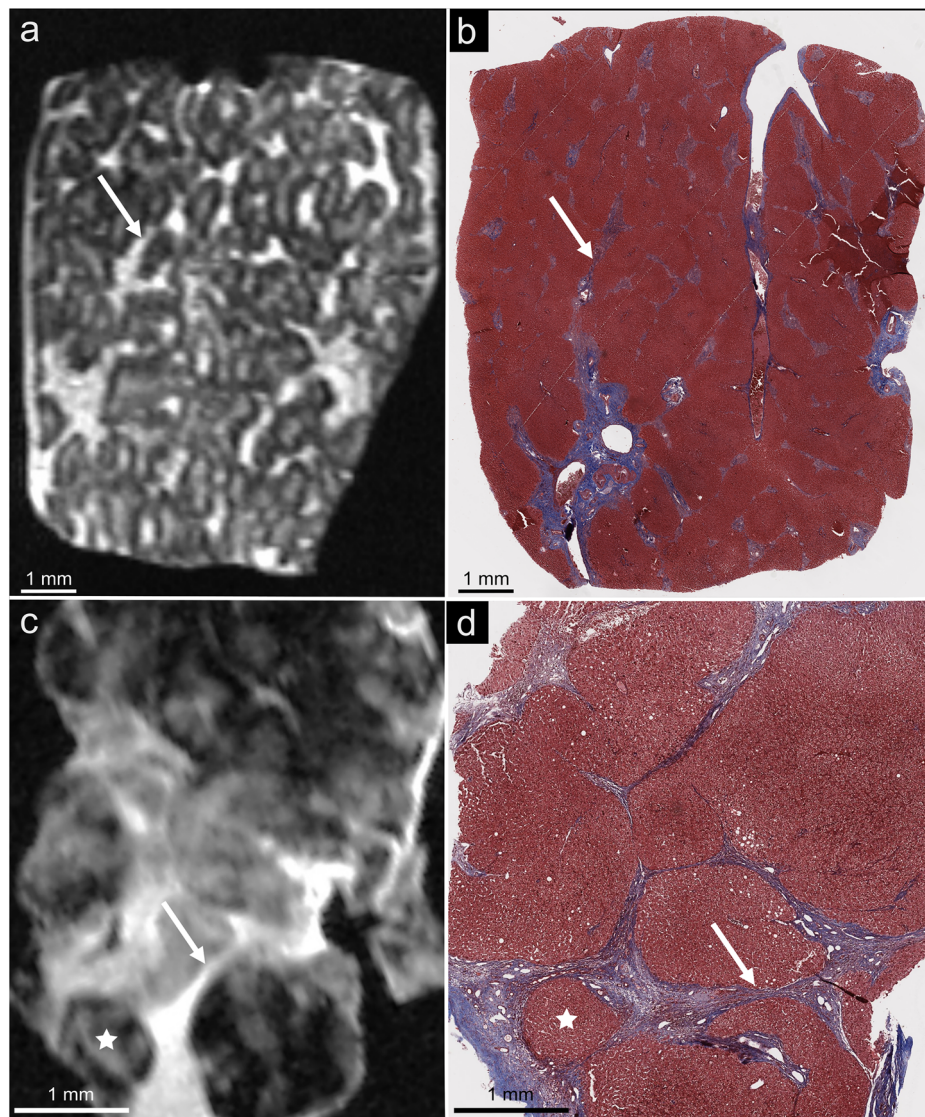
Fig. 3 Staging discrepancy between 7-T MRI and histological reference standard. 7-T MRI (**a**) was staged F2 because of early changes in the lobular architecture and rare fibrotic septa (arrow) seen between the portal spaces, while histology (**b**) was staged F3 because of numerous fibrotic septa (arrow). **c** and **d** illustrate another example where 7-T MRI (**c**) was staged F3 due to numerous fibrotic septa (arrow) while histology (**d**) was staged F4 due to regenerative nodules (star)

Additionally, volumetric images of the entire specimen could help reduce sampling errors on macroscopic evaluation of the specimens, by providing more relevant mappings than macroscopic "naked eye" analysis, to select areas to be sectioned for further histological analysis. However, the broader use of this technique as a surrogate for extemporaneous analysis has been limited by several factors, including prolonged acquisition times and the high cost and limited availability of the equipment, particularly in oncologic surgery, where perioperative decisions require rapid turnaround times. While current MRI acquisition times remain impractical for intraoperative use and/or extemporaneous examination, ongoing technological advancements, such as improved MRI coils or accelerated acquisition techniques, will hopefully significantly reduce scanning times while preserving sufficient spatial resolution and signal-to-noise ratio.

Furthermore, this method could also improve radiologists' understanding of clinical MRI, as MRI features of diseases have often been established on an empirical basis, while the underlying pathological mechanisms inducing signal changes are not always well understood. New information, such as tissue hydration or fibrosis, may become accessible and quantifiable, in addition to the

Dana *et al. European Radiology Experimental*   (2025) 9:54

Page 9 of 10

possibility of examining the entire volume of a sample without destruction [29]. In chronic liver disease, a better understanding of the normal and pathological micro-architecture of the liver parenchyma is fully in line with the current drive to develop noninvasive imaging bio-markers aiming to go beyond histopathology, aiming at replacing liver biopsies [30] but remains mostly limited to MRI elastography in fibrosis [31]. Thus, by providing unparalleled images of the liver micro-architecture, high-field MRI bridges the gap between clinical MRI and his-topathology, providing a better understanding of the anatomical basis of clinical *in vivo* MRI. However, for that purpose and without being able to use a cryoprobe with clinical MRI, major technological developments are required to translate this technique, focusing on reducing breathing and motion artifacts and improving coil design. Additionally, our MRI-based results also outline potential novel research directions, such as the use of machine learning for automated fibrosis detection.

To demonstrate that MRI could be disruptively used to provide a histopathology-like examination, we needed a model allowing qualitative and quantitative analysis. Liver fibrosis appeared as an appropriate model because of the existence of widely validated histological classifi-cations of liver fibrosis, with low subjectivity, such as the METAVIR score on Masson's trichrome-stained sections [10–15]. The METAVIR score, validated in chronic viral hepatitis, was chosen as a uniform scoring system for all cases, regardless of the aetiology of liver disease. This represents a limitation as specific features such as perisinusoidal or perivenular fibrosis in the con-text of steatohepatitis were not considered. Furthermore, no patients with chronic viral hepatitis were included. Nevertheless, it enabled a fully blinded review of the cases without bias from known chronic liver disease. Further research with a larger patient cohort and various aetiol-ogies of liver disease is required to refine our under-standing of 7-T MRI liver semiology and evaluate different liver fibrosis stages, as the impact of potential confounding factors may have been overlooked in this preliminary study.

High-field 7-T MRI provides an assessment similar to low-magnification histology (1×–2×). Beyond fibrosis staging of liver tissue, MRI enables a cross-sectional volumetric exploration of the entire specimen, without cutting or destroying the sample. With short-time image acquisition and immediate image reading, high-field MRI could become a new modality for extemporaneous tissue analysis, especially in oncologic surgery. On the other hand, future research developments should focus on bridging the gap with *in vivo* MRI to impact clinical practice and provide true noninvasive microscopic histo-logic examination.

Abbreviations

CI	Confidence interval
MRI	Magnetic resonance imaging
RARE	Rapid imaging with refocused echoes

Data availability
Data are available on demand at IHU Strasbourg (corresponding author AV).

Declarations

Ethics approval and consent to participate
This prospective project was approved by the Research Ethics Board (Protocol RIPH2, LivMod N°IDRCB 2019-A00738-49 ClinicalTrial NCT04690972) and followed ethical principles of the Declaration of Helsinki.

Consent for publication
All patients provided written informed consent.

Competing interests
AV is a member of the Scientific Editorial Board of *European Radiology Experimental* (section: Abdomen/gastrointestinal) and, as such, did not participate in the selection or review processes for this article. The remaining authors declare no conflicts of interest.

Author details
[1]Université de Strasbourg, Inserm, UMRS 1110, Institute for Translational Medicine and Liver Disease, Strasbourg, France. [2]Institute of Image-Guided Surgery - IHU Strasbourg, Strasbourg, France. [3]Department of Diagnostic Radiology, McGill University, Montreal, Canada. [4]Augmented Intelligence & Precision Health Laboratory (AIPHL), Research Institute of the McGill University Health Centre, Montreal, Canada. [5]Département de Pathologie, Hôpitaux Universitaires de Strasbourg, Strasbourg, France. [6]ICube UMR 7357, Université de Strasbourg/CNRS, Fédération de Médecine Translationnelle de Strasbourg, Strasbourg, France. [7]Département de Pathologie, Hôpital Beaujon, FHU MOSAIC, Université Paris Cité, Paris, France. [8]Département de Radiologie, Hôpital Beaujon, Université Paris Cité, Paris, France. [9]Service de Chirurgie Viscérale et Digestive, Nouvel Hôpital Civil, Hôpitaux Universitaires de Strasbourg, Strasbourg, France. [10]Pôle Hépato-digestif, Service d'Hépatogastroenterologie, Hôpitaux Universitaires de Strasbourg, Strasbourg,

Dana *et al. European Radiology Experimental*   (2025) 9:54

Page 10 of 10

France. [11]Département de Radiologie, Hôpital Américain de Paris, Paris, France. [12]Inria, Institut national de recherche en sciences et technologies du numérique, Paris, France. [13]Plateforme Imageries du Vivant, Université de Paris, PARCC, INSERM, Paris, France. [14]Department of Radiology–Medical Physics, University Hospital Freiburg, Freiburg, Germany.

References

1. Volmar KE, Idowu MO, Souers RJ et al (2015) Turnaround time for large or complex specimens in surgical pathology: a College of American Pathologists Q-Probes study of 56 institutions. Arch Pathol Lab Med 139:171–177. https://doi.org/10.5858/arpa.2013-0671-CP
2. Novis DA, Zarbo RJ (1997) Interinstitutional comparison of frozen section turnaround time. A College of American Pathologists Q-Probes study of 32868 frozen sections in 700 hospitals. Arch Pathol Lab Med 121:559–567. https://doi.org/10.5858/arpa.2013-0671-cp
3. Regev A, Berho M, Jeffers LJ et al (2002) Sampling error and intraobserver variation in liver biopsy in patients with chronic HCV infection. Am J Gastroenterol 97:2614–2618. https://doi.org/10.1002/hep.21346
4. Merriman RB, Ferrell LD, Patti MG et al (2006) Correlation of paired liver biopsies in morbidly obese patients with suspected nonalcoholic fatty liver disease. Hepatology 44:874–480. https://doi.org/10.1002/hep.21346
5. Potretzke TA, Saling LJ, Middleton WD et al (2018) Bleeding complications after percutaneous liver biopsy: do subcapsular lesions pose a higher risk? AJR Am J Roentgenol 211:204–210. https://doi.org/10.2214/ajr.17.18726
6. Baltes C, Radzwill N, Bosshard S et al (2009) Micro MRI of the mouse brain using a novel 400 MHz cryogenic quadrature RF probe. NMR Biomed 22:834–442. https://doi.org/10.1002/nbm.1396
7. Dashevsky BZ, D'Alfonso T, Sutton EJ et al (2015) The potential of high resolution magnetic resonance microscopy in the pathologic analysis of resected breast and lymph tissue. Sci Rep 5:17435. https://doi.org/10.1038/srep17435
8. Dana J, Venkatasamy A (2022) High-resolution (7-T) liver MRI for pathologic examination. Radiology 306:74–75. https://doi.org/10.1148/radiol.220410
9. Korteweg MA, Zwanenburg JJM, Hoogduin JM et al (2011) Dissected sentinel lymph nodes of breast cancer patients: characterization with high-spatial-resolution 7-T MR imaging. Radiology 261:127–135. https://doi.org/10.1148/radiol.11103535
10. Kleiner DE, Brunt EM, Van Natta M et al (2005) Design and validation of a histological scoring system for nonalcoholic fatty liver disease. Hepatology 41:1313–1321. https://doi.org/10.1002/hep.20701
11. Desmet VJ, Gerber M, Hoofnagle JH, Manns M, Scheuer PJ (1994) Classification of chronic hepatitis: diagnosis, grading and staging. Hepatology 19:1513–1520
12. Bedossa P, Poynard T (1996) An algorithm for the grading of activity in chronic hepatitis C. Hepatology 24:289–2893. https://doi.org/10.1002/hep.510240201
13. Moon AM, Singal AG, Tapper EB (2020) Contemporary epidemiology of chronic liver disease and cirrhosis. Clin Gastroenterol Hepatol 18:2650–2666. https://doi.org/10.1016/j.cgh.2019.07.060
14. Wang S, Friedman SL (2023) Found in translation—fibrosis in metabolic dysfunction–associated steatohepatitis (MASH). Sci Transl Med 15:eadi0759. https://doi.org/10.1126/scitranslmed.adi0759
15. Dana J, Venkatasamy A, Saviano A et al (2022) Conventional and artificial intelligence-based imaging for biomarker discovery in chronic liver disease. Hepatology Int 16:509–522. https://doi.org/10.1007/s12072-022-10303-0
16. Bankhead P, Loughrey MB, Fernández JA et al (2017) QuPath: open source software for digital pathology image analysis. Sci Rep 7:16878. https://doi.org/10.1038/s41598-017-17204-5
17. Kikinis R, Pieper SD, Vosburgh KG (2013) 3D Slicer: a platform for subject-specific image analysis, visualization, and clinical support. In: Jolesz FA (ed) Intraoperative imaging and image-guided therapy. Springer, New York. https://link.springer.com/chapter/10.1007/978-1-4614-7657-3_19
18. Fleiss JL, Levin B, Paik MC (2003) The measurement of interrater agreement. In: Statistical methods for rates and proportions, 3rd edn. Wiley, New York. https://doi.org/10.1002/0471445428
19. Landis JR, Koch GG (1977) The measurement of observer agreement for categorical data. Biometrics 33:159–174
20. DeRose JA, Doppler M (2018) Guidelines for understanding magnification in the modern digital microscope era. Microscopy Today 26:20–33. https://doi.org/10.1017/S1551929518000688
21. Faria SC, Ganesan K, Mwangi I et al (2009) MR imaging of liver fibrosis: current state of the art. Radiographics 29:1615–1635. https://doi.org/10.1148/rg.296095512
22. Serai SD, Trout AT, Miethke A et al (2018) Putting it all together: established and emerging MRI techniques for detecting and measuring liver fibrosis. Pediatr Radiol 48:1256–1272. https://doi.org/10.1007/s00247-018-4083-2
23. Minamikawa T, Hase E, Ichimura-Shimizu M et al (2022) Assessment of ultra-early-stage liver fibrosis in human non-alcoholic fatty liver disease by second-harmonic generation microscopy. Int J Mol Sci 23:3357. https://doi.org/10.3390/ijms23063357
24. Rousselet MC, Michalak S, Dupré F et al (2005) Sources of variability in histological scoring of chronic viral hepatitis. Hepatology 41:257–264. https://doi.org/10.1002/hep.20535
25. Ladd ME, Bachert P, Meyerspeer M et al (2018) Pros and cons of ultra-high-field MRI/MRS for human application. Prog Nucl Magn Reson Spectrosc 109:1–50. https://doi.org/10.1016/j.pnmrs.2018.06.001
26. Cardenas AM, Sarlls JE, Kwan JY et al (2017) Pathology of callosal damage in ALS: an ex-vivo, 7 T diffusion tensor MRI study. Neuroimage Clin 15:200–208. https://doi.org/10.1016/j.nicl.2017.04.024
27. Donatelli G, Emmi A, Costagli M et al (2023) Brainstem anatomy with 7-T MRI: in vivo assessment and ex vivo comparison. Eur Radiol Exp 7:71. https://doi.org/10.1186/s41747-023-00389-y
28. Harteveld AA, Denswil NP, Siero JCW et al (2016) Quantitative intracranial atherosclerotic plaque characterization at 7T MRI: an ex vivo study with histologic validation. AJNR Am J Neuroradiol 37:802–810. https://doi.org/10.3174/ajnr.a4628
29. Mankovich NJ, Robertson DR, Cheeseman AM (1990) Three-dimensional image display in medicine. J Digit Imaging 3:69–80. https://doi.org/10.1007/BF03170565
30. Yu JH, Lee HA, Kim SU (2023) Noninvasive imaging biomarkers for liver fibrosis in nonalcoholic fatty liver disease: current and future. Clin Mol Hepatol 29:S136–S149. https://doi.org/10.3350/cmh.2022.0436
31. Ajmera V, Loomba R (2021) Imaging biomarkers of NAFLD, NASH, and fibrosis. Mol Metab 50:101167. https://doi.org/10.1016/j.molmet.2021.101167

Publisher's Note

Springer Nature remains neutral with regard to jurisdictional claims in published maps and institutional affiliations.